Article Subject (see Index Terms below and write one here) Magnetodynamics

Effective Damping Constant and Current Induced Magnetization Switching of GdFeCo / TbFe Exchange-Coupled Bilayer

T. Higashide[1], B. Dai[2], T. Kato[1], D. Oshima[3], S. Iwata[3]

[1] *Department of Electric Engineering and Computer Science, Nagoya University, Nagoya, 464-8603, Japan*
[2] *Center for composite Materials and Structures, Harbin Institute of Technology, Harbin 150080, P.R.China*
[3] *Institute of Materials and Systems for Sustainability, Nagoya University, Nagoya, 464-8603 Japan*

Received 1 Apr 2015, revised 15 Apr 2015, accepted 20 Apr 2015, published 1 Jun 2015, current version 15 Jun 2015. (Dates will be inserted by IEEE; "published" is the date the accepted preprint is posted on IEEE Xplore®; "current version" is the date the typeset version is posted on Xplore®).

Abstract—Gilbert damping constant α and effective perpendicular magnetic anisotropies K_{eff} of amorphous GdFeCo (10 – x nm) / TbFe (x nm) exchange-coupled bilayer with various TbFe layer thicknesses x were measured, and the product α × K_{eff} of the bilayer was compared with a critical current density J_c of the current-induced magnetization switching (CIMS) observed for the giant magneto-resistance (GMR) nano-pillars with the GdFeCo / TbFe memory layer. The damping constant α of the bilayer, estimated by time-resolved magneto-optical Kerr effect measurements, was 0.051 for x = 0, and was significantly enhanced to 0.23 for x = 1. The anisotropy constant K_{eff} and the product M_sH_k were also confirmed to increase with increasing the TbFe thickness x. The CIMS of the GdFeCo (9 nm) / TbFe (1 nm) bilayer exhibited 1.6 times larger J_c than that of GdFeCo (10 nm), while the product α × K_{eff} was confirmed to increase by a factor of 10.

Index Terms—Amorphous magnetic materials, Gilbert damping, Magnetic anisotropy, Magnetization reversal

I. INTRODUCTION

MAGNETIC random access memory (MRAM) has many advantages, such as nonvolatility, good scalability, high endurance, and high operating speed, which make the MRAM a promising candidate for the next-generation universal memory. However, high-density MRAMs with Gbit-class capacity are required to replace the conventional memories, such as SRAM, DRAM, and Flash. Current-induced magnetization switching (CIMS) is considered to be a promising technology for realization of Gbit-class MRAM, and CIMS has been demonstrated in magnetic tunneling junctions (MTJs) with a perpendicular magnetic anisotropy (PMA) [Ikeda 2010, Nakayama 2009, Diao 2007, Hayakawa 2005, Kubota 2005]. PMA materials are quite effective for maintaining the thermal stability of the information (magnetization direction), even when cell size is small, as well as for achieving low switching current density J_c. However, challenges remain to developing high-density MRAMs with densities of several Gbit and beyond, since it will be necessary to further reduce J_c while keeping sufficient thermal stability of the memory cell.

One possible solution for this challenge is a so-called thermally assisted MRAM in which the memory layer is heated during the writing [Prejbeanu 2007, Prejbeanu 2013]. We have studied amorphous TbFe [You 2008, You 2009] and GdFeCo [Dai 2012, Dai 2013] as memory layers in thermally assisted MRAM cells, since the GdFeCo and TbFe are known to exhibit large PMA, and their magnetic properties, such as magnetization, coercivity, and Curie temperature can be easily tuned by changing their composition [Gambino 1999, Tsunashima 1982, Tsunashima 2001]. We previously demonstrated the CIMS of giant magneto-resistance (GMR) nano-pillars with a GdFeCo memory layer, and studied the compositional and temperature dependences of the critical current density J_c [Dai 2012, Dai 2013].

In this paper, we report the CIMS of GMR nano-pillars with a GdFeCo / TbFe exchange-coupled bilayer, and the variation in J_c by the insertion of TbFe with high PMA and low Curie temperature. We then report the Gilbert damping constant α and perpendicular anisotropy K_{eff} of the GdFeCo / TbFe exchange coupled bilayer. Although the J_c is known to be proportional to the product α × K_{eff}, in a single memory layer [Hayakawa 2005], the results of this paper suggest that the simple relation, $J_c \propto \alpha \times K_{eff}$ does not hold in the exchange-coupled bilayer.

II. EXPERIMENTAL METHOD

For estimations of the damping constant and PMA of the GdFeCo / TbFe exchange-coupled bilayers, samples with a stack of substrate / Ta (5 nm) / CuAl (30 nm) / Ta (3 nm) / $Tb_{16}Fe_{84}$ (x nm) / $Gd_{21}(Fe_{90}Co_{10})_{79}$ (10 – x nm) / Ta (2 nm) / SiN (40 nm) were deposited on thermally oxidized Si substrates by RF magnetron sputtering, where the TbFe thickness x was varied from 0 to 5 nm. A surface SiN layer was deposited to improve the signal-to-noise ratio on the time-

Corresponding author: T. Kato (takeshik@nuee.nagoya-u.ac.jp).
Digital Object Identifier: 10.1109/LMAG.2009.2033258 (inserted by IEEE).

resolved magneto-optical Kerr effect (TRMOKE) measurements. Hysteresis loops of the bilayer were measured by an alternating gradient field magnetometer (AGM), and the effective perpendicular anisotropy constant K_{eff} was measured using a torque magnetometer. For the CIMS experiments, GMR films with $Gd_{21}(Fe_{90}Co_{10})_{79}$ (10 – x nm) / $Tb_{16}Fe_{84}$ (x nm) memory layers were sputtered. The GMR films were microfabricated to a 120 × 180 nm^2 size by electron beam (EB) lithography, and subsequent Ar^+ ion etching. Details of the film stack and fabrication process are described in our previous papers [Dai 2012, Dai 2013]. All the measurements, including the TRMOKE described below, were conducted at room temperature.

The Gilbert damping of the bilayer was evaluated from the magnetization precession monitored by the TRMOKE using a high-power fiber laser with a wavelength of 1050 nm, a pulse width of 500 fsec, and a repetition frequency of 100 kHz. The frequency-doubled probe beam was incident normal to the film surface, and the polarization of the reflected probe beam was analyzed to monitor the perpendicular component of the magnetization after the illumination of the pump beam. The fluences of the pump and probe beams were 0.6 and 0.08 mJ/cm^2, respectively. During the measurement, a magnetic field with a maximum value of 14 kOe was applied at an angle of 40 deg from the film normal direction. The TRMOKE spectra were analyzed by a damped oscillation function, $Ae^{-t/\tau}\sin\omega t$, where t is the delay time of the probe beam with respect to the pump illumination, τ is the relaxation time, and ω is the angular frequency of the oscillation. To estimate the damping constant α and anisotropy field H_k of the bilayer, the external field dependences of the ω and τ were fitted with expressions in [Suhl 1955, Beaujour 2009].

III. RESULTS AND DISCUSSIONS

Figure 1 shows hysteresis loops taken for (a) GdFeCo (10 nm) single layer and (b) GdFeCo (9 nm) / TbFe (1 nm) bilayer. Both films exhibited perpendicular magnetic anisotropy and the easy axis of the magnetization was along the film normal direction. The saturation magnetization M_s of the bilayer was around 200 emu/cc, and did not depend significantly on the TbFe thickness, since the $Tb_{17}Fe_{83}$ (10 nm) single layer also exhibited magnetization of around 200 emu/cc (data not shown). On the other hand, the anisotropy field H_k of the bilayer significantly increased by exchange coupled to a thin TbFe layer. The H_k was estimated to be 2.9 kOe for GdFeCo (10 nm) and 7.5 kOe for GdFeCo (9 nm) / TbFe (1 nm) from Figs 1 (a) and (b), respectively. This was due to the large perpendicular anisotropy of TbFe. The TbFe single layer is known to exhibit a perpendicular anisotropy around 5 x 10^6 erg/cc, and the anisotropy field of TbFe having M_s = 200 emu/cc is estimated to be 50 kOe which is much higher than the maximum applied field of our apparatuses: the AGM and torque magnetometer.

FIG. 1 HERE

Figure 2 shows the R–I loops of the GMR nano-pillars with an (a) GdFeCo (10 nm) layer and (b) GdFeCo (9 nm) / TbFe (1 nm) bilayer as memory layers. The loops were obtained by measuring the resistance after applying the current pulse with a pulse width of 100 msec. External fields H_{ex} of (a) –830 Oe and (b) –740 Oe were applied along the film normal direction to cancel the coupling between reference and memory layers. Distinct resistance changes in Fig. 2 correspond to the full reversal of the (a) GdFeCo and (b) GdFeCo / TbFe by the CIMS. A positive current means that electrons flow from the reference layer to the memory layer, which tends to align the magnetizations of the two layers parallel (P): a low-resistance state, like that in Fig. 2, and a negative current tends to be antiparallel (AP): a high resistance state. The critical current density J_c was estimated by averaging the current densities to switch from P to AP and from AP to P, since the average value is independent of the external field H_{ex} [Dai 2012], and the J_c was 1.4 × 10^7 A/cm^2 for the (a) GdFeCo single layer and 2.2 × 10^7 A/cm^2 for the (b) GdFeCo / TbFe bilayer.

FIG. 2 HERE

Figure 3 shows the dependence of J_c on the thickness of TbFe in the GdFeCo / TbFe bilayer. The value of the effective anisotropy K_{eff}, which is the sum of the PMA constant K_u and demagnetizing energy $-2\pi M_s^2$, measured for as-deposited GdFeCo / TbFe bilayers is also shown in the figure. The J_c of the GdFeCo (9 nm) / TbFe (1 nm) was confirmed to increase by 1.6 times compared to that of the GdFeCo (10 nm), while the K_{eff} of the bilayer was nearly doubled. The unequal gains of J_c and K_{eff} in the exchange-coupled bilayer may be an intriguing feature in terms of the effective increase of thermal stability of the memory layer, while keeping J_c low, which is crucial to achieve high-density MRAMs.

FIG. 3 HERE

In order to discuss the unequal gains of J_c and K_{eff} in the bilayer, the Gilbert damping constant of the GdFeCo / TbFe bilayers, which is known as a parameter to determine the J_c, was estimated by TRMOKE measurements. Figure 4 shows the decaying magnetization precessions of the GdFeCo (10 – x nm) / TbFe (x nm) bilayer (x = 0, 1) under various external fields H_{ex}. The raw data, measured by the TRMOKE, contain the signals of laser-induced demagnetization at t = 0, and exponential decay due to the recovery of magnetization as described in [Kato 2008]. These unnecessary signals were subtracted to extract the decaying precession triggered by the pump illumination, as shown in Fig. 4. We kept the pump fluence as low as possible to avoid the influence of the thermal effect on the estimated results. The typical laser-induced demagnetization at t = 0 was several percentage points of the total magnetization. Open circles and solid lines show measured data and fitted curves with the damped oscillation function, $Ae^{-t/\tau}\sin\omega t$, respectively. A clear

oscillation due to the magnetization precession of the GdFeCo can be seen in Fig. 4 (a), and the oscillation frequency increased with increasing H_{ext}. On the other hand, the precession of GdFeCo (9 nm) / TbFe (1 nm) was confirmed to relax much faster than that of GdFeCo. The g-factor and anisotropy field H_k were estimated by fitting the H_{ex} dependence of ω shown in Fig. 5 (a) with the expression in [Suhl 1955], and the damping constant α was estimated using the slope of the ω dependence of 1 / τ shown in Fig. 5 (b) with the expression $1 / \tau = \alpha \omega + \Delta\omega$. For the GdFeCo (10 nm), these values were g = 2.2, α = 0.051, and H_k = 2 kOe. All these parameters are known to be sensitive to the composition of rare earth elements, and their values were roughly consistent with the previous reports [Kato 2008, Komiya 2010]].

FIG. 4 HERE

FIG. 5 HERE

The relaxation time τ estimated from TRMOKE is known to be enhanced by inhomogeneity of the anisotropy [Rossing 1963], spin pumping [Tserkovnyak 2002], and two-magnon scattering [Sparks 1961]. The contribution from the inhomogeneity of the anisotropy ΔH_k of the bilayers, which is proportional to f_0 in the above expression [Rossing 1963], was excluded by the linear fit of the data shown in Fig. 5 (b).

The effect of spin pumping in capping and buffer Ta layers is considered to be negligibly small [Mizukami 2001, Kato 2011], and light elements Cu and Al also do not contribute spin pumping due to their small spin orbit coupling [Tserkovnyak 2005]. In addition, the contribution of the two-magnon scattering is considered to be negligible. The inhomogeneity ΔH_k of the bilayer is quite small compared to the anisotropy field H_k, which can be seen from the small $\Delta\omega$ in Fig. 5 (b), and ΔH_k would be at most 100 Oe, resulting in a negligibly small contribution to the estimation of α [McMichael 2004]. The small ΔH_k reflects good homogeneity of the sample since the amorphous GdFeCo and TbFe have uniform magnetic properties applicable to magneto-optical recording media [Tsunashima 2001]. In this experiment, we applied an external field along 40 deg from the film normal during TRMOKE measurements, and the perpendicular anisotropy of the bilayer tended to shift its magnetization slightly to the film normal direction. For the magnetization angle from the film normal, φ < 45 deg, the two-magnon contribution will be further reduced from that in the case of φ = 90 deg [McMichael 2004]. The exclusion of the two-magnon scattering was also supported by the difference of the TbFe thickness dependences on α (or τ) and H_k, which we discuss later. The two-magnon contribution to τ is expected to be proportional to H_k^2 [McMichael 2004], since the inhomogeneity ΔH_k, is considered to be proportional to H_k.

Figure 6 (a) shows the TbFe thickness dependence of the damping constant α of the GdFeCo(10 – x nm) / TbFe (x nm) bilayer. The damping constant α of the GdFeCo / TbFe was relatively low 0.051 for x = 0, and increased significantly to 0.23 for x = 1. TbFe thickness dependence of the anisotropy field H_k estimated from the TRMOKE measurements is shown in Fig. 6 (b). The H_k gradually increased with increasing TbFe thickness up to 0.5 nm, then rapidly increased above a TbFe thickness of 0.5 nm. The H_k estimated from TRMOKE agreed well with the H_k estimated from the hysteresis loops measured by AGM (see Fig. 1). The estimated g-factor of all the bilayers was around 2.2 (not shown).

The α (or τ) gradually increased at TbFe thickness x from 0 to 0.5 nm, while H_k was not significantly increased in this thickness region, as shown in Figs. 6 (a) and (b). The significant increase of α in the GdFeCo / TbFe bilayer shown in Fig. 6 (a) may be related to the large orbital moment of the 4f electrons in Tb. The large orbital moment of Tb is considered to be a source of the large PMA in the TbFe since the large orbital moment corresponds to non-spherical electron clouds of Tb, which couples strongly to neighboring atoms. However, the large electrostatic coupling to neighboring atoms results in a large α due to the energy dissipation from spin to lattice during the magnetization precession. Besides the fast relaxation process mentioned above, a slow relaxation process which is a consequence of the anisotropy of the exchange interaction between conduction electrons and 4f magnetic moments may be important [Woltersdorf 2009], since our bilayers are metals not oxides. Both these processes could explain the significant enhancement of the damping of α by impurities of rare earth with large orbital moments. For a TbFe single layer, no magnetization precession was observed (not shown), which indicates that the TbFe single layer has a quite large α. Similarly, increases of α were reported in (GdRE)FeCo alloy films, in which Gd was partly replaced by other rare earth elements, RE = Tm or Er [Komiya 2010]. In the (GdRE)FeCo, a mere 3–10 % substitution of Tm or Er for Gd was reported to result in a roughly 3–6-fold increase of α.

FIG. 6 HERE

We compared the product $\alpha \times M_s H_k$ ($\alpha \times K_{eff}$) of the as-deposited GdFeCo / TbFe bilayers with the J_c of CIMS as shown in Fig. 6 (c), since the J_c is known to be proportional to the product, $\alpha \times K_{eff}$, in a single memory layer. The M_s and H_k were estimated from hysteresis loops of the bilayers as shown in Fig. 1. The K_{eff} was measured by a torque magnetometer, and the product $M_s H_k$ agreed well with 2 K_{eff}. Figure 6 (c) plots both $\alpha \times M_s H_k$ (open circles) and $\alpha \times K_{eff}$ (closed circles) were plotted, which was normalized so that the value for GdFeCo (10 nm) was unity.

As discussed in Fig. 3, the J_c of the GdFeCo (9 nm) / TbFe (1 nm) was confirmed to increase 1.6 times compared to that of the GdFeCo (10 nm), while the product $\alpha \times K_{eff}$ was confirmed to increase by a factor of 10. This suggests that an empirical relation, $J_c \propto \alpha \times K_{eff}$, does not hold in the exchange-coupled bilayer system. We compared the K_{eff} and J_c of a $Gd_x(FeCo)_{100-x}$ single layer in our previous studies [Dai 2012, Dai 2013], and reported a roughly proportional relationship between K_{eff} and J_c of GdFeCo with various Gd contents.

There would be an additional contribution from the change in damping constant with the Gd content, but we expected the difference of the damping constant to be less than double from our previous studies [Kato 2008, Komiya 2010], which means the relation $J_c \propto \alpha \times K_{eff}$ holds in the single memory layer. Further studies on the dynamical response of the exchange-coupled bilayer are needed to elucidate the phenomena observed in this paper. For example, at this stage, we did not consider the thermal effects due to the large switching current density J_c in CIMS, the effect of dipole / exchange coupling between memory and reference layers to the damping constant of the memory layer, etc. However, from the observed quite large difference in gains between J_c and $\alpha \times K_{eff}$ by exchange coupling to TbFe, we consider the exchange-coupled bilayer to be an attractive option for realizing high-density MRAM with both low J_c and high thermal stability.

IV. CONCLUSIONS

Gilbert damping constants α and effective PMA K_{eff} of the GdFeCo (10 – x nm) / TbFe (x nm) exchange-coupled bilayers with various TbFe layer thicknesses x were measured, and the product $\alpha \times K_{eff}$ of the bilayer was compared with J_c of the CIMS observed for the GMR nano-pillars with the GdFeCo / TbFe memory layer. The α of the GdFeCo single layer estimated by TRMOKE was 0.051, and increase of the TbFe layer thickness resulted in an increase of α to 0.23 for x = 1. By CIMS experiments, the J_c of the GdFeCo (9 nm) / TbFe (1 nm) was confirmed to increase 1.6 times compared to that of the GdFeCo (10 nm). On the other hand, the $\alpha \times K_{eff}$ was confirmed to increase by a factor of 10, which was much larger than the increase of J_c, indicating the quite large difference in gains between J_c and $\alpha \times K_{eff}$ using the GdFeCo / TbFe exchange-coupled bilayer. Thus we consider the exchange coupled bilayer to be an attractive to option for realizing high density MRAM with both low J_c and high thermal stability.

ACKNOWLEDGMENT

The authors would like to thank Mr. M. Kumazawa of Nagoya University for his assistance in the experiments. The authors are grateful for financial support in the form of a Grand-in- Aids for Scientific Research from the Ministry of Education, Culture, Sports, Science and Technology, and funds from SCOPE from the Ministry of Internal Affairs, and the Hibi Science Foundation.

REFERENCES

Ikeda S, Miura K, Yamamoto H, Mizunuma K, Gan H D, Endo M, Kanai S, Hayakawa J, Matsukura F, Ohno H (2010), "A perpendicular anisotropy CoFeB-MgO magnetic tunnel junction," Nat. Mater., vol. 9, pp. 721-724, doi:10.1038/nmat2804.

Nakayama M, Kai T, Shimomura N, Amano M, Kitagawa E, Nagase T, Yoshikawa M, Kishi T, Ikegawa S, Yoda H (2009), "Spin transfer switching in TbCoFe / CoFeB / MgO / CoFeB / TbCoFe magnetic tunnel junctions with perpendicular magnetic anisotropy," J. Appl. Phys., vol. 103, 07A710, doi: 10.1063/1.2838335.

Diao Z, Li Z, Wang S Y, Ding Y, Panchula A, Chen E, Wang L C, Huai Y (2007), "Spin-transfer torque switching in magnetic tunnel junctions and spin-transfer torque random access memory," J. Phys.: Condens. Matter., vol. 19, 165209, doi: 10.1088/0953-8984/19/16/165209.

Hayakawa J, Ikeda S, Lee Y M, Sasaki R, Meguro T, Matsukura F, Takahashi H, Ohno H (2005), "Current-Driven Magnetization Switching in CoFeB / MgO / CoFeB Magnetic Tunnel Junctions," Jpn. J. Appl. Phys., vol. 44, pp. L1267-L1270, doi: 10.1143/JJAP.44.L1267.

Kubota H, Fukushima A, Ootani Y, Yuasa S, Ando K, Maehara H, Tsunekawa K, Dyayaprawira D D, Watanabe N, Suzuki Y (2005), "Evaluation of Spin-Transfer Switching in CoFeB / MgO / CoFeB Magnetic Tunnel Junctions," Jpn. J. Appl. Phys., vol. 44, pp. L1237-L1240, doi: 10.1143/JJAP.44.L1237.

Prejbeanu I L, Kerekes M, Sousa R C, Sibuet H, Redon O, Dieny B, Nozières J P (2007), "Thermally assisted MRAM". J. Phys.: Cond. Mat. vol. 19, 165218, doi: 10.1088/0953-8984/19/16/165218.

Prejbeanu I L, Bandiera S, Alvares-Hérault J, Sousa R C, Dieny B, Nozières J P (2013), "Thermally assisted MRAMs: ultimate scalability and logic functionalities," J. Phys. D: Appl. Phys., vol. 46, 074002, doi: 10.1088/0022-3727/46/7/074002.

You L, Kato T, Tsunashima S, Iwata S (2008), "Dynamic Heating in Micron- and Submicron-Patterned TbFe films," Jpn. J. Appl. Phys., vol. 47, pp. 146-149, doi: 10.1143/JJAP.47.146.

You L, Kato T, Tsunashima S, Iwata S (2009), "Thermomagnetic writing on deep submicron-patterned TbFe films by nanosecond current pulse," J. Magn. Magn. Mater., vol. 321, pp. 1015-1018, doi: 10.1016/j.jmmm.2008.10.026.

Dai B, Kato T, Iwata S, Tsunashima S (2012), "Spin Transfer Torque Switching of Amorphous GdFeCo with Perpendicular Magnetic Anisotropy for Thermally Assisted Magnetic Memories," IEEE Trans. Magn., vol. 48, pp. 3223-3226, doi: 10.1109/TMAG.2012.2196988.

Dai B, Kato T, Iwata S, Tsunashima S (2013), "Temperature Dependence of Critical Current Density of Spin Transfer Torque Switching Amorphous GdFeCo for Thermally Assisted MRAM," IEEE Trans. Magn., vol. 49, pp. 4359-4362, doi: 10.1109/TMAG.2013.2240380.

Gambino R J, Suzuki T (1999), *Magneto-optical Recording Materials*, 1st ed., New York: IEEE PRESS, pp. 33-42.

Tsunashima S, Masui S, Kobayashi T, Uchiyama S (1982), "Magneto-optic Kerr effect of amorphous Gd-Fe-Co films," J. Appl. Phys., vol. 53, pp. 8175-8177, doi: 10.1063/1.330283.

Tsunashima S (2001), "Magneto-optical recording," J. Phys. D Appl. Phys., vol. 34, pp. R87-R102, doi: 10.1088/0022-3727/34/17/201.

Suhl H (1955), "Ferromagnetic resonance in nickel ferrite between one and two kilomegacycles," Phys. Rev., vol. 97, pp. 555-557, doi: 10.1103/PhysRev.97.555.2.

Kato T, Nakazawa K, Komiya R, Nishizawa N, Tsunashima S, Iwata S (2008), "Compositional Dependence of g-Factor and Damping Constant of GdFeCo Amorphous Alloy Films," IEEE Trans. Magn., vol. 44, pp. 3380-3383, doi: 10.1109/TMAG.2008.2001679.

Komiya R, Kato T, Nishizawa N, Tsunashima S, Iwata S (2010), "Compositional dependence of g-factor and damping constant of $(Gd_{100-x}RE_x)$FeCo alloy films (RE = Yb, Tm, Er)," J. Phys.: Conf. Ser., vol. 200, 04202, doi: 10.1088/1742-6596/200/4/042010.

Rossing T D (1963), "Resonance linewidth and anisotropy variation in thin films," J. Appl. Phys., vol. 34, p. 995, doi: 10.1063/1.1729582.

Tserkovnyak Y, Brataas A, Bauer G E W (2002), "Enhanced Gilbert damping in thin ferromagnetic films," Phys. Rev. Lett., vol. 88, 117601, doi: 10.1103/PhysRevLett.88.117601.

Sparks M, Loudon R, Kittel C (1961), " Ferromagnetic relaxation. I. Theory of the relaxation of the uniform precession and the degenerate spectrum in insulators at low temperature," Phys. Rev., vol. 122, pp. 791-803, doi: 10.1103/PhysRev.122.791.

Mizukami S, Ando Y, Miyazaki T (2001), "The study on ferromagnetic resonance linewidth for NM/80NiFe/NM (NM = Cu, Ta, Pd, and Pt) films," Jpn. J. Appl. Phys., vol. 40, pp. 580-585, doi: 10.1143/JJAP.40.580.

Kato T, Matsumoto Y, Okamoto S, Kikuchi N, Kitakami O, Nishizawa N, Tsunashima S, Iwata S (2011), "Time-resolved magnetization dynamics and damping constant of sputtered Co/Ni multilayers," IEEE Trans. Magn., vol. 47, pp. 3036-3039, doi: 10.1109/TMAG.2011.2158082.

Tserkovnyak Y, Brataas A, Bauer G E W, Halperin B I (2005), "Nonlocal magnetization dynamics in ferromagnetic heterostructures," Rev. Mod. Phys., vol. 77, pp. 1375-1421, doi: 10.1103/RevModPhys.77.1375.

McMichael R D, Krivosik P (2004), "Classical model of extrinsic ferromagnetic resonance linewidth in ultrathin films," IEEE Trans. Magn., vol. 40, pp. 2-11, doi: 10.1109/TMAG.2003.821564.

De Gennes P G, Kittel C, Portis A M (1959), "Theory of ferromagnetic resonance in rare earth garnets. II. Line widths," Phys. Rev., vol. 116, pp. 323-330, doi: 10.1103/PhysRev.116.323.

Woltersdorf G, Kiessling M, Meyer G, Thiele J -U, Back C H (2009), "Damping by slow relaxing rare earth impurities in Ni80Fe20," Phys. Rev. Lett., vol. 102, 257602, doi: 10.1103/PhysRevLett.102.257602.

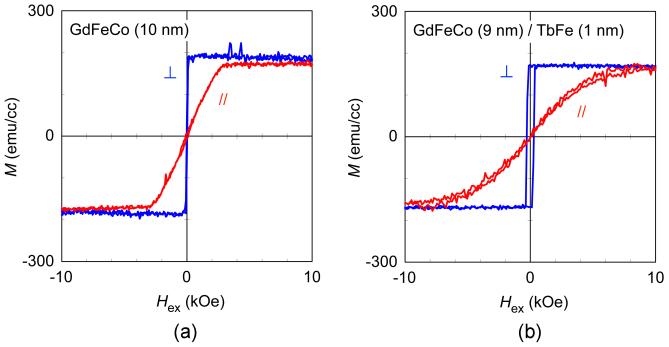

Fig. 1. Hysteresis loops taken for (a) GdFeCo (10 nm) single layer, and (b) GdFeCo (9 nm) / TbFe (1 nm) bilayer. The loops were taken by applying a magnetic field perpendicular (⊥) and parallel (//) to the film plane.

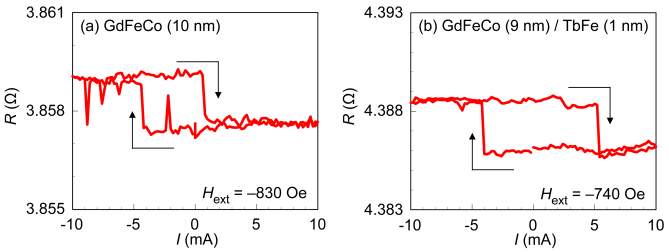

Fig. 2. *R–I* loops of GMR nano-pillars with (a) GdFeCo (10 nm), and (b) GdFeCo (9nm) / TbFe (1nm) memory layers. The loops were obtained by measuring the resistance after applying the current pulse with a pulse width of 100 msec, and external fields H_{ext} of (a) –830 Oe, and (b) –740 Oe were applied to cancel the coupling between memory and reference layers.

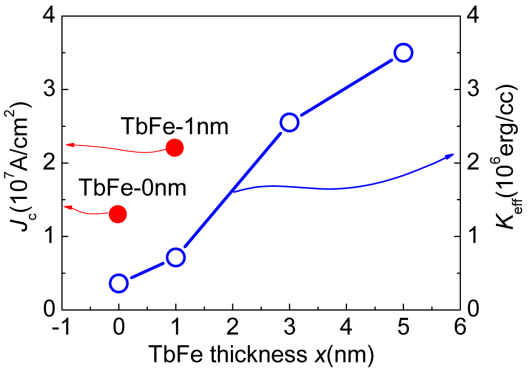

Fig. 3. TbFe thickness dependence of J_c estimated for the GMR nano-pillars with GdFeCo (10 – *x* nm) / TbFe (*x* nm) bilayers. The value of the effective anisotropy K_{eff} measured for as-deposited GdFeCo / TbFe bilayers is also shown.

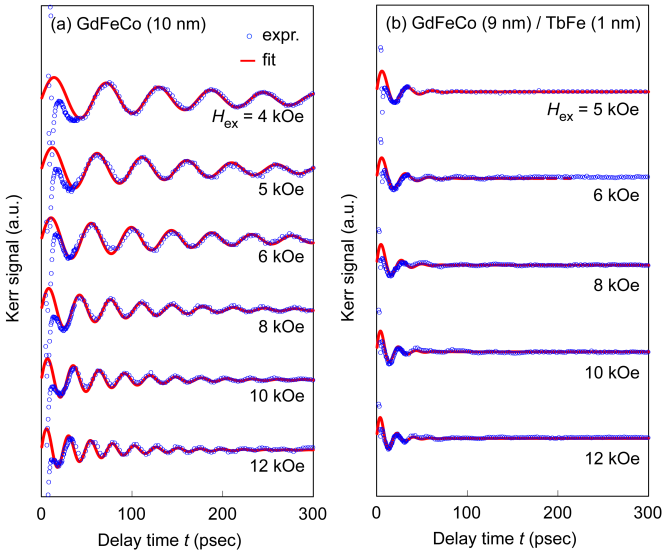

Fig. 4. Decaying magnetization precessions of the GdFeCo (10 – *x* nm) / TbFe (*x* nm) bilayer (*x* = (a) 0, (b) 1) under various external fields H_{ex} probed by TRMOKE. The unnecessary signals, laser-induced demagnetization at *t* = 0, and exponential decay due to the recovery of magnetization were subtracted to extract the decaying precession.

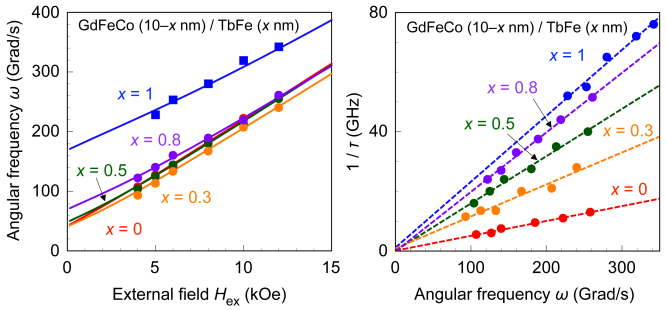

Fig. 5. (a) H_{ex} dependence of angular frequency ω and (b) ω dependence of 1 / τ of GdFeCo (10 – x nm) / TbFe (x nm) bilayers. ω and τ were estimated from the TRMOKE signals shown in Fig. 4. The solid lines in Fig. (a) are fitted curves using the expression described in [Suhl 1955] to estimate g-factor and H_k. The dashed lines in Fig. (b) represent linear fits of the data to estimate damping constant α.

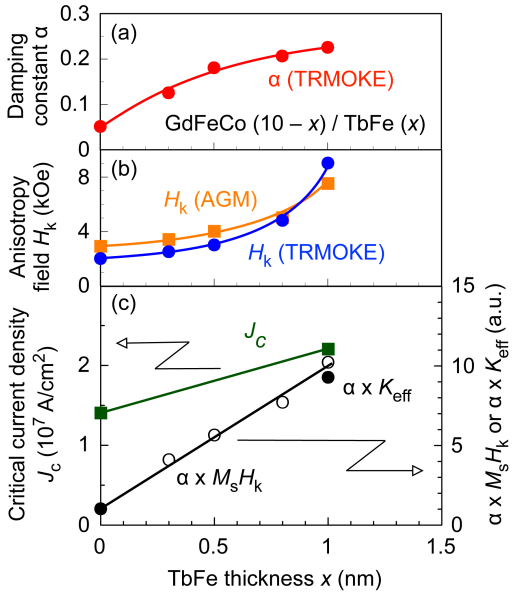

Fig. 6. (a) TbFe thickness dependence of the damping constant α of the GdFeCo / TbFe bilayer; (b) TbFe layer thickness dependence of the anisotropy field H_k estimated from TRMOKE and AGM; (c) TbFe thickness dependence of the critical current density J_c of the GMR nanopillars with GdFeCo / TbFe bilayers and the product α × K_{eff} of the bilayers.